



Published in final edited form as:

RSC Adv. ; 4(14): 7185–7192. doi:10.1039/C3RA44137G.

Covalent Immobilization of Collagen on Titanium through Polydopamine Coating to Improve Cellular Performances of MC3T3-E1 Cells

Xiaohua Yu¹, John Walsh², and Mei Wei^{1,*}

¹Department of Materials Science and Engineering, University of Connecticut Storrs, CT, 06269, USA

²Department of Molecular and Cell Biology, University of Connecticut, Storrs, Connecticut 06269, USA

Abstract

Surface modification of orthopedic implants is critical for improving the clinical performance of these medical devices. Herein, collagen was covalently immobilized onto a titanium implant surface via a novel adherent polydopamine coating inspired by mussel adhesive proteins. The formation and composition of the collagen coating was characterized using X-ray photoelectron spectroscopy (XPS) and scanning electron microscopy (SEM). Fluorescent labeled collagen was also used to examine the formation and uniformity of the collagen coating. The resultant collagen coating with a polydopamine supporting substrate demonstrated better uniformity and distribution on the titanium surface compared to a physical adsorption of collagen. The covalent immobilized collagen coating is biologically active, as evidenced by its ability to enhance MC3T3-E1 cell adhesion, support cell proliferation and promote early stage osteogenic differentiation of pre-osteoblasts. Our study suggests covalent immobilization of collagen through the polydopamine coating might be an efficient way to improve the cellular performance of implant surfaces.

1. Introduction

Titanium and its alloys have been used in dental and orthopedic fields for decades due to their excellent mechanical properties, good resistance to corrosion and inertness in physiological environment[1–3]. However, titanium based implants often fail to form direct bonding at the bone-to-implant interface, which can cause severe issues such as implant loosening for patients during the tenure of implantation [4,5]. In order to improve the initial stability of bone-contacting implants, a variety of surface modification technologies have been explored to enhance the direct bone bonding between the native bone and the implant [6–9]. A common approach to modify the implant surface is to immobilize bioactive molecules, such as application of proteins and peptides onto material surfaces [7,10]. Although physical adsorption of biomolecules has shown its simplicity and flexibility, it largely suffers from its instability and lack of quality control [11]. This is mainly due to the

Corresponding author: Mei Wei, Ph. D, Department Materials Science and Engineering, University of Connecticut, 97 North Eagleville Road, U-3136, Storrs, CT, 06269, USA, Tel: 1-860-486-9253, Fax: 1-860-486-4745, meiwei@enr.uconn.edu.

fact that passive adsorption through electrostatic interactions is usually reversible. The coatings can be easily removed post implantation [12]. Thus, robust coating with a long-term stability is highly desirable in the context of material surface modification for implants.

Covalent immobilization of biomolecules on material surfaces is through a chemical conjugation between the substrate and the target biomolecule [13]. Compared to passive physical adsorption, this approach possesses several distinct advantages when it is used as a surface modification strategy [14]. First of all, covalent attachment of molecules can improve substantially the stability of the resultant coatings through its irreversible manner. Besides, covalent immobilization also offers better control over coating fabrication parameters such as coating thickness, ligand density, and molecular orientation [15–17]. Recently, a mussel-inspired surface functionalization technique developed by Messersmith et al. has shown its universal applicability to form strong adhesive interaction with various material surfaces [18]. More importantly, polydopamine, the main component of this technique exhibits high reactivity towards biomolecules containing amine and thiol functional groups [19,20]. Thus, the polydopamine coating might be a promising approach for development of optimum metallic implants.

Collagen as the major organic component of bone extracellular matrix is frequently used to improve cellular activity, such as adhesion, proliferation and differentiation on biomaterials surfaces [21–25]. Although numerous strategies have developed to immobilize collagen onto titanium surface to improve the biocompatibility of the implants, most of these methods involve complicated chemistry which usually introduce extra toxic factors onto the targeted surface [26,27]. In this study, we successfully adapt the mussel-inspired polydopamine chemistry to address the issue of collagen immobilization in the biomaterial field. A two-step approach was developed on the surface of the titanium implants: polydopamine coating was firstly introduced onto the titanium surface then followed by covalent coupling with fibrillar type I collagen. We then particularly focus on the effect of collagen immobilization on pre-osteoblast attachment, expansion and differentiation as each of these outputs is closely related to the biocompatibility of the implants.

Materials and methods

2.1 Collagen immobilization on substrate

Commercially available titanium disks (15 mm in diameter, 0.2 mm in thickness) were used as substrates in this study. These disks were polished by #800 sandpaper and ultrasonically cleaned using acetone, ethanol and de-ionized water, respectively. Dopamine (Sigma, MO) was dissolved at a concentration of 2 mg/mL in 10 mM Tris-HCl (pH=8.5). The titanium disks were soaked in the dopamine solution for 18 h at room temperature. The dopamine-coated substrates (DOPA-Ti) were then collected and rinsed with de-ionized water and air dried at room temperature. Collagen was isolated from rat tails and stored at 4 °C as described elsewhere [28]. To couple the collagen onto the DOPA-Ti, 1.0 mL 100 µg/mL collagen was mixed with EDC (10 mM) and NHS (25 mM) in de-ionized water. DOPA-Ti was immersed in the collagen/EDC/NHS solution for 48 h at 4 °C to immobilize collagen onto the titanium, namely COL-DOPA. Collagen was also coated on Ti surfaces without polydopamine coating under the same condition and used as a control, namely COL-Ti.

Both collagen coated surfaces were subsequently rinsed with de-ionized water and dried at 37 °C for 30 min. All the samples were stored at 4 °C until further experiments.

2.2 Characterization of collagen coating

The morphology of the coating surface with different compositions was observed using field emission scanning electron microscopy (FESEM, JEOL 6335F, Japan) at 5 KV. The surface composition of coated surface was analyzed using X-ray photoelectron spectroscopy (XPS) with a PHI multiprobe with Mg as the exciting source. The XPS survey spectra were obtained using pass energy of 100 eV and energy step size of 1 eV, and the high resolution XPS spectra data were collected using pass energy of 50 eV and energy step size of 0.1 eV. The quantitative compositional analysis was carried out using CasaXPS fitting program and based on the collected XPS data. All binding energies were referred to the C1s neutral carbon peak at 284.6 eV.

2.3 Visualization of collagen coating via fluorescence tagging

For fluorescent labeling, 5(6)-carboxyrhodamine 6G (Sigma, MO) was conjugated using NHS/DIC chemistry. The resultant product was purified by dialysis against de-ionized water using a dialysis unit with MWCO=1000. The rhodamine labeled collagen (Rho-COL) was used to visualize collagen immobilization onto DOPA-Ti surfaces. Briefly, Rho-COL (100 µg/mL) solution was mixed with EDC (10 mM) and NHS (25 mM) in de-ionized water. The coated titanium disks (DOPA-Ti) were immersed in the above Rho-collagen solution for 48 h at 4 °C. Titanium disks without dopamine coating were used as a control. After extensive washing with de-ionized water, the Rho-COL on the the surface of Ti disks was visualized using a fluorescence microscope (Zeiss Axiovert 200M) with a TRITC filter.

2.4 Cell culture

MC3T3-E1 cells were cultured in alpha minimum essential medium (α -MEM) supplemented with 10% FBS (Cellgro) and 1% pen-strep (Cellgro). Cells were grown in a humidified atmosphere of 5% CO₂ at 37 °C. The culture medium was changed every other day. An osteogenic medium, consisting of α -MEM plus 10 mM β -glycerol phosphate and 50 µg/mL L-ascorbic acid (Sigma, MO), was used after the cells grew onto the coatings for 1 week. Sub-confluent cells were harvested from the flask and seeded onto four different substrates: Ti (untreated titanium), DOPA-Ti, COL-Ti and COL-DOPA. The seeding density of the cells on all substrates was 2.0×10^4 cells/cm² in a 24-well plate. The medium was changed after 8 h of seeding and all the samples were transferred to a new plate to remove all the unattached cells.

2.5 MC3T3-E1 cells viability and ALP assay

Cell viability was analyzed at day 3, 7, and 14 using the Alamar Blue assay. At each time point, the culture medium was aspirated and the samples were rinsed with PBS. Fresh medium (0.5 mL) containing 10% Alamar Blue dye (Biosource International) was added to each well and subsequently incubated for 2 h. The incubated medium was measured by a microplate reader (Biotek, MQX200) at wavelengths of 570 and 600 nm. The analytical assays were performed at each of time point with replicates of 5 samples per group.

The activity of alkaline phosphatase (ALP) was measured as described previously [9]. Briefly, at each time point, the cells were washed with PBS and lysed with 1 mL lysis buffer containing 0.5% Triton X-100 for 20 min. The cell lysis was then centrifuged at 3000 rpm at 4 °C for 10 min. Aliquots of supernatants were subjected to a total protein assay using a BCA assay kit (Thermo Scientific). The ALP activity was measured by colorimetric assay with reagent mixture composed of 5 mM *p*-nitrophenol phosphate disodium (*p*-NPP), 1 mM MgCl₂, and 0.15 M 2-amino-2-methyl-1-propanol (AMP) (Sigma, MO) together with an equal volume amount of nitrophenyl phosphate (10 mM). The optical density of the solution was measured at 405 nm using a microplate reader (Biotek, MQX200). The ALP activity was expressed as total protein per microgram protein per sample.

2.6 Immunocytochemistry

MC3T3-E1 cells were seeded onto COL-Ti and COL-DOPA surfaces in a 24-well plate at a final density of 1.0×10^4 cells/cm². After 12 h and 24 h cultured in medium, cells were fixed by 4% paraformaldehyde in PBS for 20 min at room temperature. Cells were permeabilized in 0.5% Triton X-100 in PBS for 15 min, then blocked to prevent non-specific antibody adsorption using 1% FBS in PBS. After blocking, Anti-vinculin antibody (Sigma, MO) was diluted at a ratio of 1:128 and incubated with cells for 1 h at 37 °C. After thorough rinses using PBS, the cells were incubated with a goat-anti-mouse-IgG-FITC-conjugated secondary antibody (1:150, Sigma, USA). To detect actin and nucleus simultaneously, tetramethylrhodamine isothiocyanate (TRITC)-conjugated phalloidin (1:400, Invitrogen, USA) and 0.5 µg/mL 4',6-diamidino-2-phenylindole dihydrochloride (DAPI) were added in the secondary antibody solution. Cells were imaged using a fluorescent microscope (Zeiss Axiovert 200M) with filters appropriate for FITC, TRITC and DAPI.

2.7 Scanning electron microscopy

Cells were seeded onto COL-Ti and COL-DOPA plates in a 24-well plate at a density of 1.0×10^4 cells/cm². After 12 h, the cells were fixed in 2.5% glutaraldehyde/PBS for 1 h and incubated in 0.1 M sodium cacodylate buffer for another hour. The fixed cells were then dehydrated in graded ethanol series and followed by a supercritical point drying. All the samples were sputter-coated with gold palladium. Finally, the cell morphology on different collagen coatings was examined using FESEM (LEO/Zeiss DSM 982) at 3 KV.

2.8 Mineralization of collagen coated surface *in vitro*

Simulated body fluid (SBF) was prepared as reported previously [29]. The reagents were added to de-ionized water at the following order and concentration: 142 mM NaCl, 5 mM KCl, 1.5 mM MgCl₂, 0.5 mM MgSO₄, 150 mM NaHCO₃, 20 mM Tris, 2.5 mM CaCl₂, and 1.0 mM Na₂HPO₄. The pH of m-SBF was adjusted to 7.40 using HCl/NaOH at 37 °C. All four groups of untreated and treated titanium disks were immersed in 50 mL SBF in a conical tube, respectively. The SBF was refreshed every day to maintain the constant ionic strength. After that, the specimens were gently washed with de-ionized water and air dried. The formation of apatite coating on the surface of titanium disks was then observed using FESEM (JEOL 6335F, Japan) at 5 KV.

2.9 Statistical analysis

All quantitative data were given as mean \pm standard deviation. The numerical results obtained in this study were subjected to a two-tailed Student's *t*-test. The significance of the results was evaluated at a significance level of $p < 0.05$ based on the *p* value of comparison.

Results

3.1 Chemical Composition

The chemical composition differences of the titanium sample before and after treatment were analyzed by XPS. Fig. 1 shows the wide scan spectra of XPS for the four treated surfaces in this study: (i) Ti, (ii) DOPA-Ti, (iii) COL-Ti, and (iv) COL-DOPA. Compared to pure titanium surface (Ti), C, O and N peaks were also observed but Ti2p peaks disappeared on the DOPA-Ti surface. The DOPA-Ti spectra indicate that a homogeneous coating was formed and fully covered titanium surface. After coupling with collagen solution, the composition of the coating changed substantially. All the peaks observed on DOPA-Ti were also observed on COL-DOPA, but both the carbon and nitrogen peaks increased significantly. The quantitative compositional analysis showed that the atomic percentage of C, N and O on COL-DOPA is 68.77%, 13.73%, and 17.50% respectively, which is very close to the theoretical atomic ratio of collagen (Table 1) [30]. In contrast, when collagen was directly immobilized on the titanium surface, although increases in C and N peak intensity were observed on the COL-Ti surface, Ti2p from titanium substrate was clearly shown on the surface, indicating the lack of uniformity of collagen coating.

3.2 Collagen coating morphology and distribution

The morphology of collagen coated surfaces was examined using SEM (Fig. 2). Compared to non-treated Ti, the DOPA-Ti surface was smoother but covered with certain amount of polydopamine precipitate residue after washing (Fig. 2 DOPA-Ti). No collagen fiber was identified on the titanium surface coated directly with collagen (COL-Ti) (Fig. 2-COL-Ti). However, collagen nanofibers were clearly seen on COL-DOPA surfaces. The diameter of the nano-sized collagen fibers is around 150–200 nm which is the typical size of collagen nanofibers in the body [31]. It is known that the d-banding pattern of collagen fibers is the characteristic structure of well assembled collagen nanofiber [32]. Collagen bundles with organized d-banding were clearly shown on the polydopamine coated titanium surface (Fig. 2-COL-DOPA). In addition, these reassembled collagen nanofibers evenly covered more than 80% of the surface.

Rhodamine-tagged collagen was used to study the distribution of collagen coating on titanium surface in addition to SEM observations. Fig. 3 shows the fluorescence images of Ti and DOPA-Ti surfaces coupled with Rho-COL. After extensive washing with de-ionized water, only scattered fluorescent signal was seen on the surface of the COL-Ti (Fig. 3-A). In contrast, large area of fluorescence with even distribution was observed on the COL-DOPA surface, suggesting a robust coupling of collagen with dopamine (Fig. 3-B). To further compare the efficiency of collagen immobilization on different substrates, half of the titanium disk was masked during polydopamine coating formation while the other half remained as pure titanium. It was found that there was almost no noticeable Rho-COL on

the half disk without the polydopamine coating, but the other half with the coating showed good coverage of Rho-COL with a strong fluorescent intensity (Fig. 3-C). To quantify the relative amount of Rho-COL on the two types of surfaces, the image was then converted to binary format (Fig. 3-D) and the signal of fluorescence was quantified (Fig. 3-E&F). The area covered by Rho-COL on COL-DOPA is 10-fold of that on COL-Ti (Fig. 3-E). The total fluorescence intensity of COL-DOPA was also 6.5 times higher than COL-Ti (Fig. 3-F).

3.3 Cell adhesion and morphology

The immunostaining of vinculin and actin was employed to visualize and evaluate cell adhesion on the collagen coated surfaces. Immunofluorescence staining showed better adhesion of MC3T3-E1 cells on COL-DOPA than COL-Ti (Fig. 4). The cells on COL-DOPA surface exhibited greater spread with organized actin into stress fibers (Fig. 4-COL-DOPA). Vinculin staining showed focal adhesion had started to form at the periphery of the cells on COL-DOPA, while the cells on COL-Ti exhibited a more slim shape with less spread (Fig. 4-COL-Ti). Cell morphologies on different surfaces were revealed by FESEM. MC3T3-E1 cells attached closely to both surfaces (Fig. 5-A & B). However, it was observed that the cells spread more cytoplasmic extensions and filopodia on COL-DOPA surface than on COL-Ti at a high magnification (Fig. 5-C & D, white arrows).

3.4 Cell proliferation and differentiation

To determine the effect of collagen immobilization on MC3T3-E1 cell proliferation, cell number on different treated surfaces were recorded at day 3, 7 and 14. They increased significantly in all tested groups as culture time was extended (Fig. 6). At day 3, although the cell number on DOPA-Ti and COL-Ti was slightly higher than that on Ti, no significant differences were found between the Ti and the COL-DOPA group. In contrast, the cell number on COL-DOPA increased more than three folds at day 7 while it only increased one fold on Ti surface. At day 14, the cell number on all treated groups was higher than the untreated Ti group. No statistical difference was found among the three treated groups.

ALP activity was evaluated as an early marker of osteogenic differentiation of MC3T3-E1 cells [33]. Although ALP activity in all groups was very low at day 3, it was noticed that ALP on COL-DOPA was still slightly higher than Ti group (Fig. 7). ALP activity on each surface increased gradually between 3 and 7 days and both collagen coated surfaces showed high ALP activity. A dramatic increase in ALP activity was observed during the second week of culture due to the switch of medium from basal medium to osteogenic medium. Although the ALP activity on Ti surfaces increased over 10 folds, the ALP activity on the treated surfaces were still significantly higher than the control. Noticeably, the expression of ALP on COL-DOPA was found to be statistically higher than COL-Ti ($p < 0.05$), which indicates the covalent immobilization approach used here is more favorable for osteogenic differentiation of cells.

3.5 *In vitro* mineralization of collagen coated surface

The four tested titanium surfaces were incubated in SBF to test their mineralization capability *in vitro*. No apatite formation was observed on the untreated titanium surface (Fig. 8-A). A homogenous layer of apatite was formed on the surface of DOPA-Ti indicating

polydopamine coating induced mineralization on titanium surface (Fig. 8-B). As for the two collagen coated titanium surfaces, scattered apatite islands with a diameter around 3 μm were found on COL-Ti while a full coverage of apatite was obtained on COL-DOPA. However, no noticeable difference was found in term of mineralization between DOPA-Ti and COL-DOPA since polydopamine is a strong apatite formation inducer [34].

Discussion

Surface modification allows the modulation of implant performances without sacrificing the physical properties of the bulk material, such as mechanical properties, porosity, and structure[35]. It is highly desirable to create implant surfaces with improved cellular performances such as cell adhesion, proliferation and material-guided differentiation [17]. In this report, the biocompatibility of titanium surfaces was enhanced by immobilization of collagen via a bioinspired approach, namely leveraging the polydopamine coating. The covalent immobilization of collagen on titanium surface through a two-step coupling improved the uniformity and stability of the collagen coating. As a result of that, the cell adhesion on the titanium surface was significantly enhanced compared to the collagen coating from simply physical adsorption. Furthermore, the presence of covalently immobilized collagen coating also promoted pre-osteoblast proliferation and strengthened the osteogenic differentiation of the cells. Thus, the mussel inspired polydopamine coating strategy provides a potential alternative for improvement of the surface properties of various implant materials.

Dopamine contains catechol and amine groups, which polymerizes at basic pH to form thin films on various material surfaces due to the excellent adhesive properties [18]. The formation of polydopamine coating on titanium has been confirmed by XPS analyses of the materials surfaces (Fig. 1). The absence of Ti2p peak from DOPA-Ti surface indicates that the polydopamine coating completely has covered the titanium surface, which would also in turn improve the uniformity of subsequent collagen coating (Fig. 2&3). More importantly, polydopamine coating exhibits strong reactivity towards various nucleophiles with amine and thiol groups due to the presence of quinone after polymerization [3637]. Thus, proteins containing large amounts of amine and thiol groups have been successfully conjugated through polydopamine coating for various applications, such as enzyme immobilization and stem cell manipulation [3839]. Covalent immobilization of collagen onto titanium surfaces was achieved by coupling collagen with a preformed polydopamine coating with the aid of EDC and NHS. The formation of bioactive collagen coating was confirmed by both the surface compositional analysis and the cell behavior test. It was found that the composition of COL-DOPA matches well with the pure collagen composition (Table. 1), indicating the full coverage of collagen on top of the polydopamine coating. Similar results were also obtained when rhodamine-tagged collagen was used for immobilization. The coverage of collagen coating visualized by fluorescence tagging was much homogenous compared to the physical adopted collagen coating (Fig. 3).

The adhesion of MC3T3-E1 cells on the COL-DOPA surface was improved significantly compared to on COL-Ti (Fig. 4&5). The enhanced cell adhesion might be attributed to the successful immobilization of well reassembled collagen nanofibers. Collagen is one of the

major ECM proteins containing numerous cell binding sites such as RGD sequences [22]. It is crucial to have sufficient adhesive ligands present on the surface of the implant to trigger cell-substrate interactions [40]. The well-organized collagen nanostructure on COL-DOPA mimics the native status of collagen which may be able to stimulate a strong adhesion triggered signaling pathway (Fig. 2). When collagen was physically adsorbed onto the titanium surface, the adsorption of collagen is not stable and can be reversible at certain extent [23,27]. Besides, the XPS results indicate that the collagen coating formed by adsorption is not homogeneous, and thus did not cover the entire titanium surface (Fig. 1). In contrast, covalent immobilization of collagen may not only improve the uniformity of the coating coverage, but also provide more precise control over the molecule to be coated such as its fouling, orientation and availability to cells [41]. Therefore, covalent collagen immobilization facilitated by polydopamine coating is a better approach to optimize the surface properties of titanium implants to enhance cell signaling and adhesion.

Collagen coating by covalent immobilization well supports MC3T3-E1 cell expansion and induces early stage osteogenic differentiation of the cells on the modified titanium surface. Compared to unmodified titanium, the cell proliferation is largely enhanced on all the treated groups including DOPA-Ti. This result indicates that the polydopamine immobilization approach is biocompatible and does not introduce toxic materials to the implant surface. This might be attributed to the excellent biocompatibility nature of the polydopamine coating (Fig. 6). Jeong et al. immobilized polydopamine on PMMA surface and observed remarkable increase in cell attachment and proliferation [39]. Similar results were also reported by Yang et al. when human umbilical vein endothelial cells (HUVEC) were seeded on a dopamine coated stainless steel surface [38]. In addition, the impact of collagen immobilization on MC3T3-E1 differentiation was more profound. ALP expression on collagen coated surfaces was higher than the two groups of collagen-free surfaces, which indicates that presence of collagen might have encouraged osteogenic differentiation of pre-osteoblasts (Fig. 7).

Furthermore, COL-DOPA groups showed stronger ALP expression compared COL-Ti with regarding to ALP expression at day 14 (Fig. 7). It has been reported that specific control over collagen distribution, orientation and reassembly could substantially affect the effectiveness of collagen coating on material surfaces [42]. Collagen immobilized through polydopamine coating has generated better collagen coverage on the titanium surface (Figs. 2 and 3). In addition, these soluble collagen molecules have successfully reassembled into well-organized nanofibers which better mimic the native structure of ECM. The improved cell adhesion resulted from this feature might result in earlier and stronger osteogenic differentiation by triggering the adhesion-induced signaling pathway [43]. In addition, the immobilized collagen also successfully supported titanium surface mineralization which is one of the prerequisites for bone contacting implants (Fig. 8). Although the presence of polydopamine on the surface might play a role during the mineralization *in vitro* [18], more uniform apatite coating was found on both DOPA-Ti and COL-DOPA compared to COL-Ti. Combining the biological data shown earlier, our study suggests surface modification through polydopamine initiated collagen immobilization.

Conclusion

In summary, a simple and efficient method has been developed to covalently immobilize type I collagen onto titanium implants. The collagen was coupled onto titanium surface through a two-step polydopamine coating approach. The resultant collagen coating showed improved uniformity and distribution on the material surfaces compared to the simply physical adsorption approach. Importantly, the covalently coated collagen promoted pre-osteoblast adhesion and subsequently enhanced cell proliferation and early stage osteogenic differentiation. Therefore, the approach described here may represent an enabling strategy to improve the performances of titanium-based implants by surface modification.

Acknowledgement

The authors would like to thank the National Science Foundation (BES 0503315 and CBET-1133883) and the NIH (R21AR059962) for their support of the research. We would acknowledge Dr. Heng Zhang at the University of Connecticut for his technical support on XPS. The authors acknowledge Dr. David W. Rowe for providing the cell line used in this study.

References

1. Geetha M, Singh AK, Asokamani R, Gogia AK. *Prog. Mater. Sci.* 2009; 54:397–425.
2. Khang D, Lu J, Yao C, Haberstroh KM, Webster TJ. *Biomaterials.* 2008; 29:970–983. [PubMed: 18096222]
3. Olivares-Navarrete R, Hyzy SL, Hutton DL, Erdman CP, Wieland M, Boyan BD, Schwartz Z. *Biomaterials.* 2010; 31:2728–2735. [PubMed: 20053436]
4. Le Guéhennec L, Soueidan A, Layrolle P, Amouriq Y. *Dent. Mater.* 2007; 23:844–854. [PubMed: 16904738]
5. Rostoker W, Galante JO. *Biomaterials.* 1981; 2:221–224. [PubMed: 7326316]
6. Liu XY, Chu PK, Ding CX. *Mater. Sci. Eng. R-Reports.* 2004; 47:49–121.
7. Castner DG, Ratner BD. *Surf. Sci.* 2002; 500:28–60.
8. Yu X, Wang L, Jiang X, Rowe D, Wei M. *J. Mater. Sci. Mater. Med.* 2012; 23:2177–2186. [PubMed: 22639151]
9. Yu X, Wei M. *J. Biomed. Mater. Res. Part B Appl. Biomater.* 2011; 97B:345–354. [PubMed: 21432993]
10. Tirrell M, Kokkoli E, Biesalski M. *Surf. Sci.* 2002; 500:61–83.
11. Schuler M, Trentin D, Textor M, Tosatti SG. *Nanomedicine (Lond).* 2006; 1:449–463. [PubMed: 17716147]
12. Luginbuehl V, Meinel L, Merkle HP, Gander B. *Eur J Pharm Biopharm.* 2004; 58:197–208. [PubMed: 15296949]
13. Costa F, Carvalho IF, Montelaro RC, Gomes P, Martins MCL. *Acta Biomater.* 2011; 7:1431–1440. [PubMed: 21056701]
14. Morra M, Cassinelli C, Cascardo G, Cahalan P, Cahalan L, Fini M, Giardino R. *Biomaterials.* 2003; 24:4639–4654. [PubMed: 12951007]
15. Jal PK, Patel S, Mishra BK. *Talanta.* 2004; 62:1005–1028. [PubMed: 18969392]
16. Nanci A, Wuest JD, Peru L, Brunet P, Sharma V, Zalzal S, McKee MD. *J. Biomed. Mater. Res.* 1998; 40:324–335. [PubMed: 9549628]
17. VandeVondele S, Voros J, Hubbell JA. *Biotechnol Bioeng.* 2003; 82:784–790. [PubMed: 12701144]
18. Lee H, Dellatore SM, Miller WM, Messersmith PB. *Science (80-).* 2007; 318:426–430.
19. Lee H, Rho J, Messersmith PB. *Adv. Mater.* 2008; 20:1–4.

20. Lee H, Lee Y, Statz AR, Rho J, Park TG, Messersmith PB. *Adv. Mater.* 2008; 20:1619–1623. [PubMed: 22228925]
21. Cen L, Liu W, Cui L, Zhang W, Cao Y. *Pediatr. Res.* 2008; 63:492–496. [PubMed: 18427293]
22. Abraham LC, Zuena E, Perez-Ramirez B, Kaplan DL. *J. Biomed. Mater. Res. - Part B Appl. Biomater.* 2008; 87:264–285. [PubMed: 18386843]
23. Van Den Dolder J, Jansen JA. *J. Biomed. Mater. Res. - Part A.* 2007; 83:712–719.
24. Yu X, Xia Z, Wang L, Peng F, Jiang X, Huang J, Rowe D, Wei M. *J. Mater. Chem.* 2012; 22:9721–9730.
25. Xia Z, Yu X, Jiang X, Brody HD, Rowe DW, Wei M. *Acta Biomater.* 2013; 9:7308–7319. [PubMed: 23567944]
26. Puleo D. *Biomaterials.* 1996; 17:217–222. [PubMed: 8624398]
27. Muller R, Abke J, Schnell E, Macionczyk F, Gbureck U, Mehrl R, Ruszczak Z, Kujat R, Englert C, Nerlich M, Angele P. *Biomaterials.* 2005; 26:6962–6972. [PubMed: 15967497]
28. Yu X, Wang L, Peng F, Jiang X, Xia Z, Huang J, Rowe D, Wei M. *J. Tissue Eng. Regen. Med.* 2012 Accepted.
29. Kokubo T, Takadama H. *Biomaterials.* 2006; 27:2907–2915. [PubMed: 16448693]
30. Parenteau-Bareil R, Gauvin R, Berthod F. *Materials (Basel).* 2010; 3:1863–1887.
31. Weiner S, Traub W, Wagner HD. *J. Struct. Biol.* 1999; 126:241–255. [PubMed: 10475685]
32. Harris JR, Reiber A. *Micron.* 2007; 38:513–521. [PubMed: 17045806]
33. Sabokbar A, Millett PJ, Myer B, Rushton N. *Bone Min.* 1994; 27:57–67.
34. Ryu J, Ku SH, Lee H, Park CB. *Adv. Funct. Mater.* 2010; 20:2132–2139.
35. Hench LL, Wilson J. *Science (80-.)*. 1984; 226:630–636.
36. Dalsin JL, Hu B-H, Lee BP, Messersmith PB. *J. Am. Chem. Soc.* 2003; 125:4253–4258. [PubMed: 12670247]
37. Yang K, Lee JS, Kim J, Bin Lee Y, Shin H, Um SH, Kim JB, Park KI, Lee H, Cho S-W. *Biomaterials.* 2012; 33:6952–6964. [PubMed: 22809643]
38. Yang Z, Tu Q, Zhu Y, Luo R, Li X, Xie Y, Maitz MF, Wang J, Huang N. *Adv. Healthc. Mater.* 2012; 1:548–559. [PubMed: 23184789]
39. Jeong KJ, Wang L, Stefanescu CF, Lawlor MW, Polat J, Dohlman CH, Langer RS, Kohane DS. *Soft Matter.* 2011; 7:8305.
40. Chang E-J, Kim H-H, Huh J-E, Kim I-A, Seung Ko J, Chung C-P, Kim H-M. *Exp. Cell Res.* 2005; 303:197–206. [PubMed: 15572039]
41. Ye Q, Zhou F, Liu W. *Chem. Soc. Rev.* 2011; 40:4244–4258. [PubMed: 21603689]
42. Thakkar H, Davey CL, Medcalf EA, Skingle L, Craig AR, Newman DJ, Price CP. *Clin. Chem.* 1991; 37:1248–1251. [PubMed: 1855297]
43. Lee YJ, Ko JS, Kim HM. *Biomaterials.* 2006; 27:3738–3744. [PubMed: 16530826]

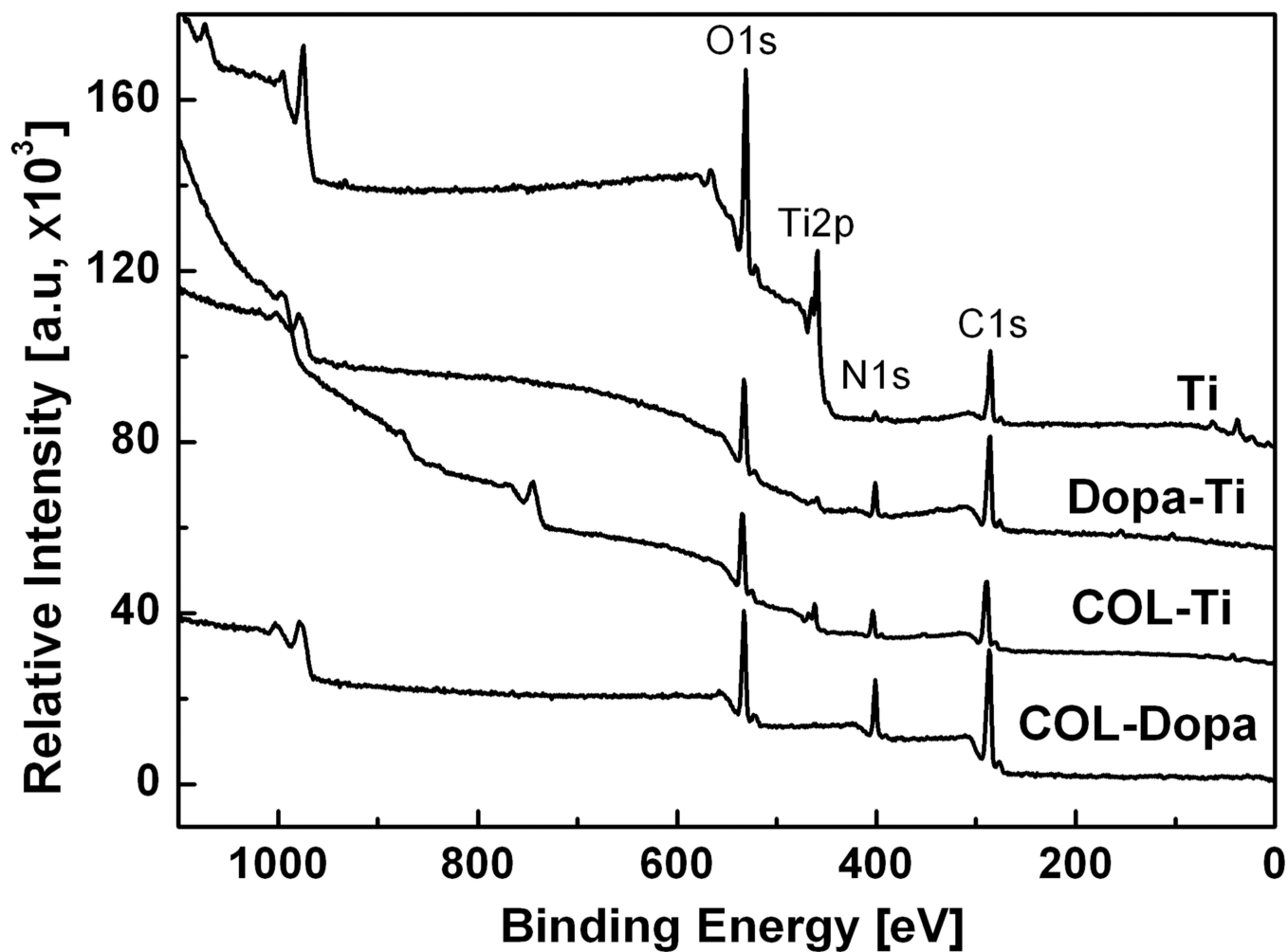


Fig. 1.

Typical XPS survey spectra of four surfaces studied: The DOPA-Ti spectra indicated a homogeneous coating was formed and fully covered the titanium surface (DOPA-Ti). After coupling with collagen solution, type I collagen coating was formed on top of the polydopamine coating (COL-DOPA).

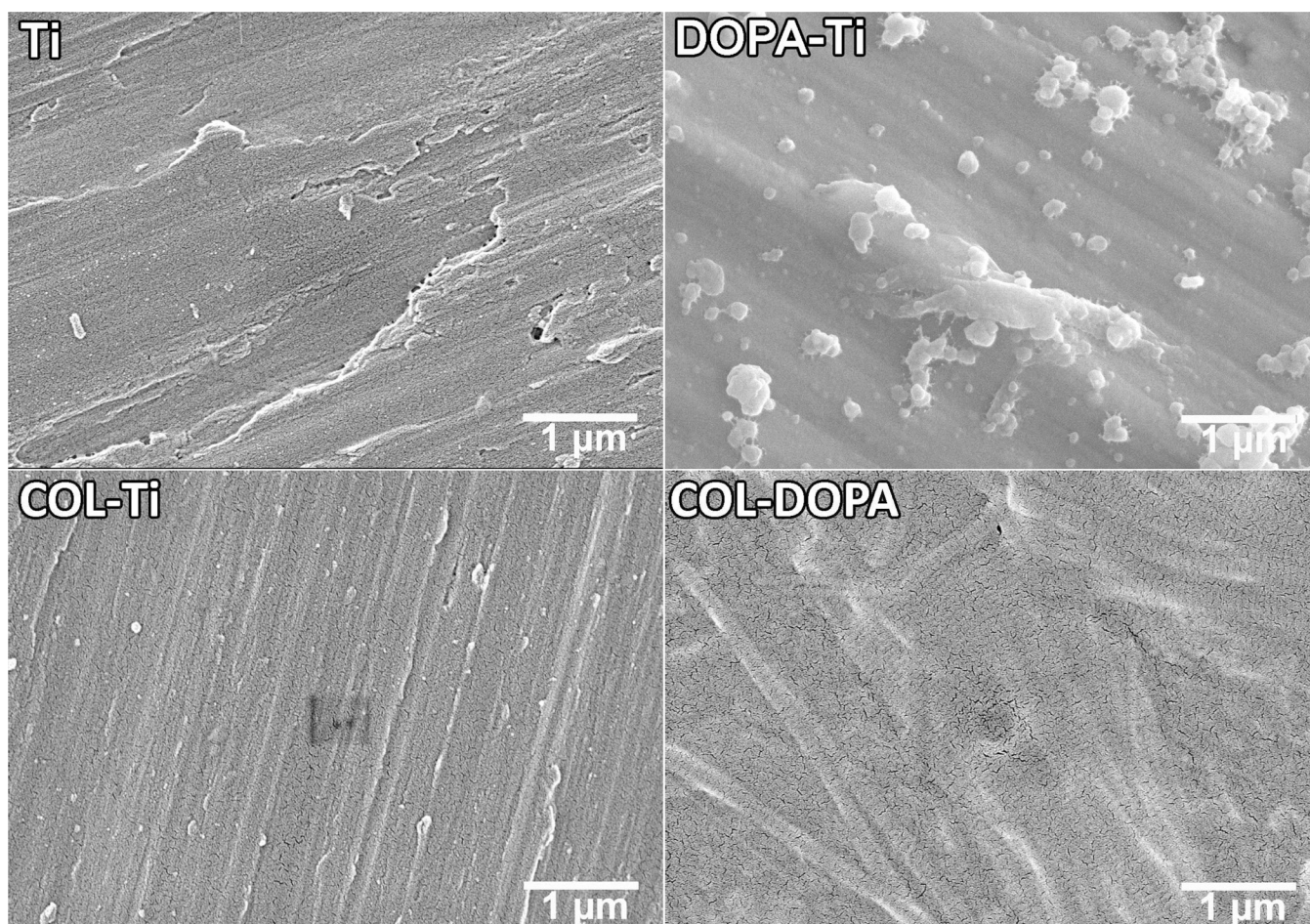


Fig. 2. SEM micrographs of the four types of titanium surfaces with different treatment: No collagen fibers were found on COL-Ti while collagen nanofibers are clearly seen on COL-DOPA surfaces. The diameter of the nano-size collagen fibers is around 150–200 nm which is the typical size of collagen nanofiber in human body.

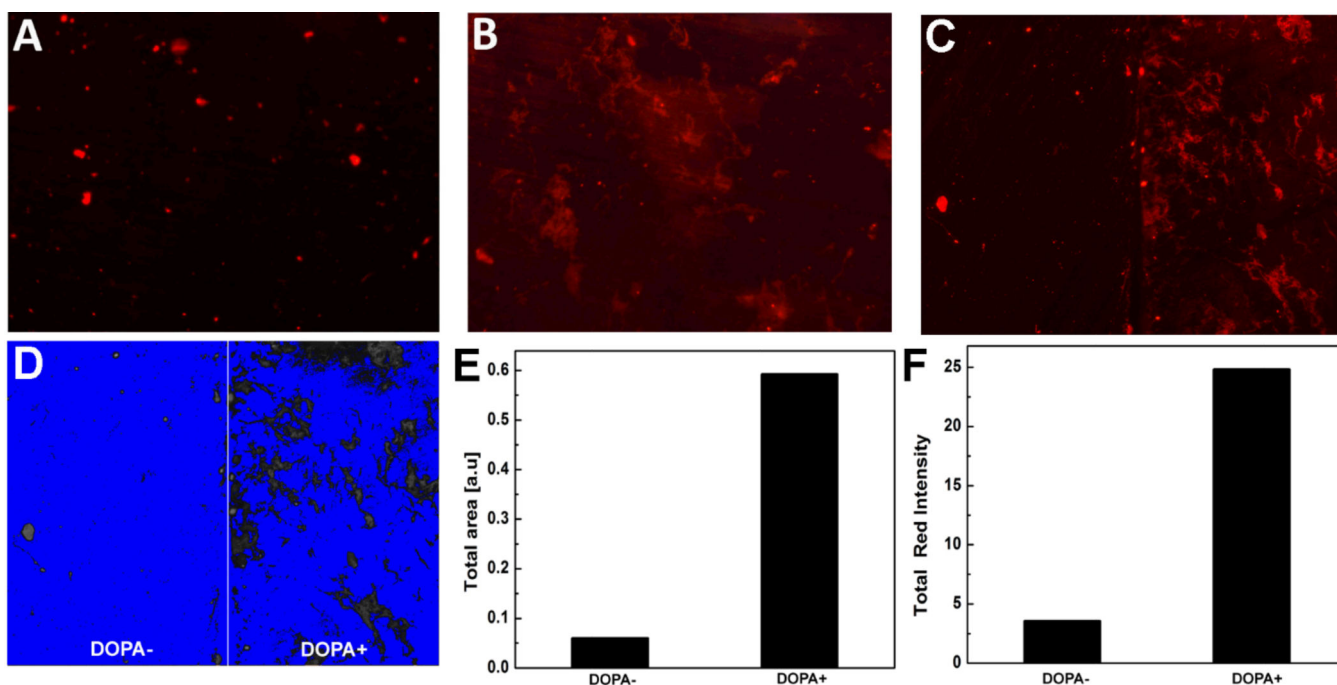


Fig. 3. Analysis of collagen immobilization on titanium surface using rhodamine tagged collagen: (A) COL-Ti, (B) COL-DOPA, and (C) Collagen coating on the same titanium disk: (-DOPA) without polydopamine treatment, (+DOPA) with polydopamine treatment, (D) Binary image of (C) for fluorescence quantification, (E) Total area of Rho-COL coverage measured by Image J, and (F) Total fluorescence intensity of Rho-COL coverage measured by Image J

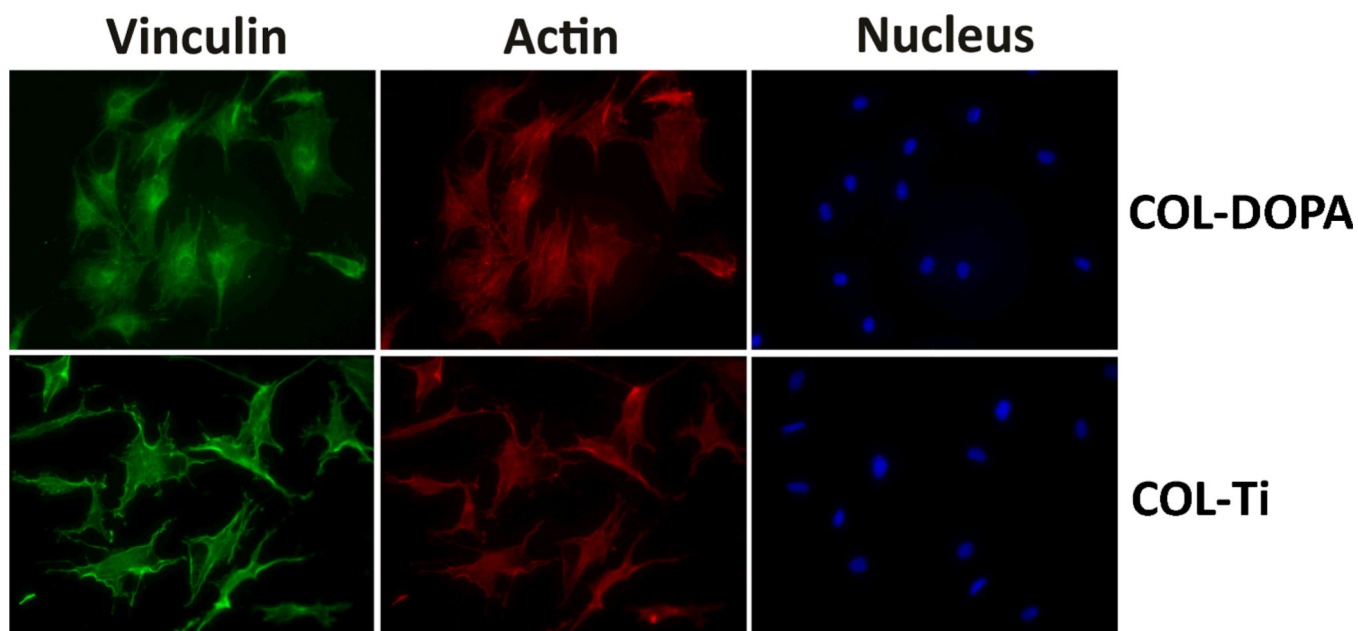


Fig. 4. Immunostaining of MC3T3-E1 cells on collagen coating prepared with different approaches: Green-Vinculin, Red-Actin, and Blue-Nucleus

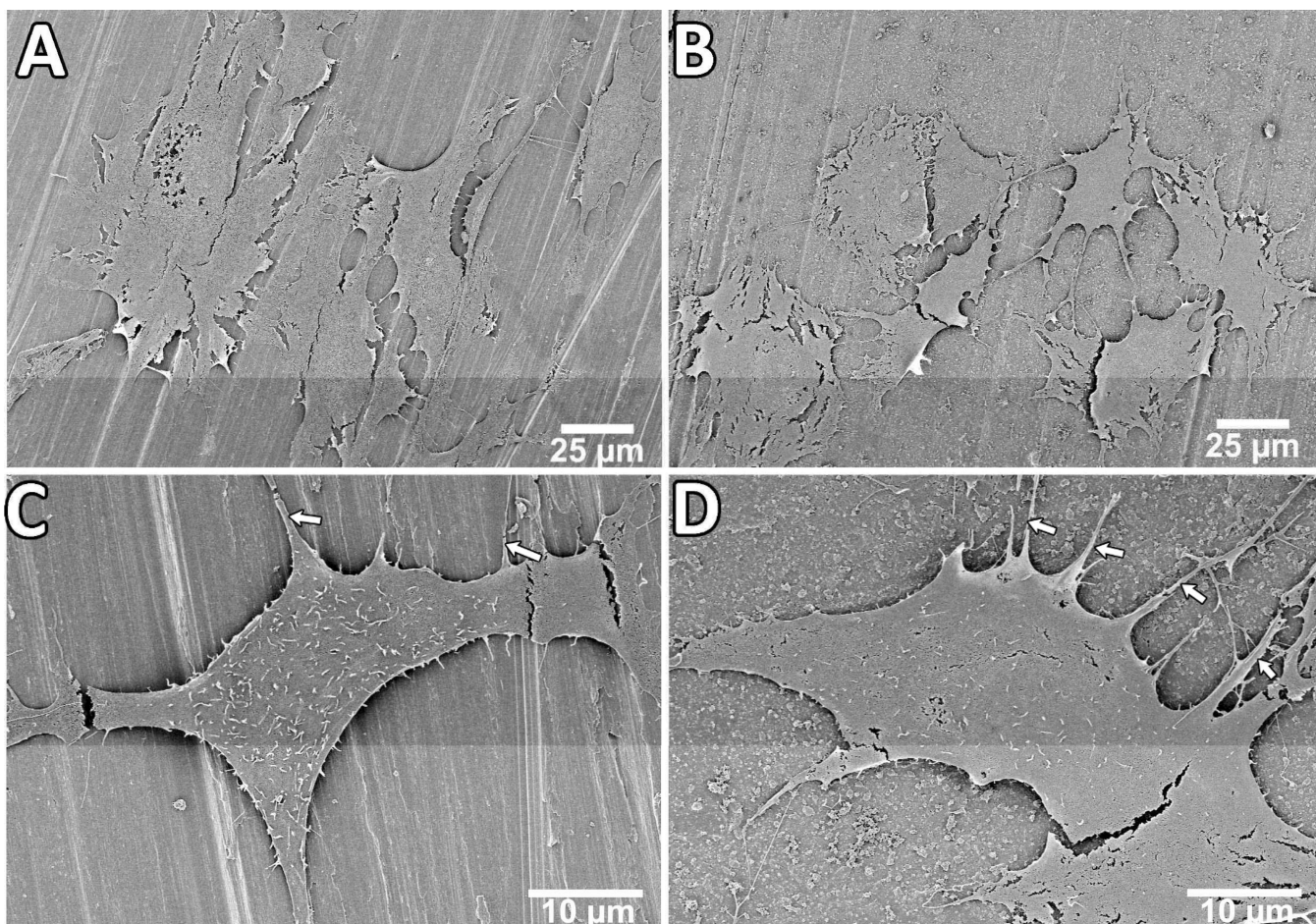


Fig. 5. SEM micrographs showing MC3T3-E1 cell morphology cultured on type I collagen coated surface after 24 h adhesion: (A) COL-Ti \times 500, (B) COL-DOPA \times 500, (C) COL-Ti \times 2000, (D) COL-DOPA \times 2000, white arrows indicates filopodia of cells.

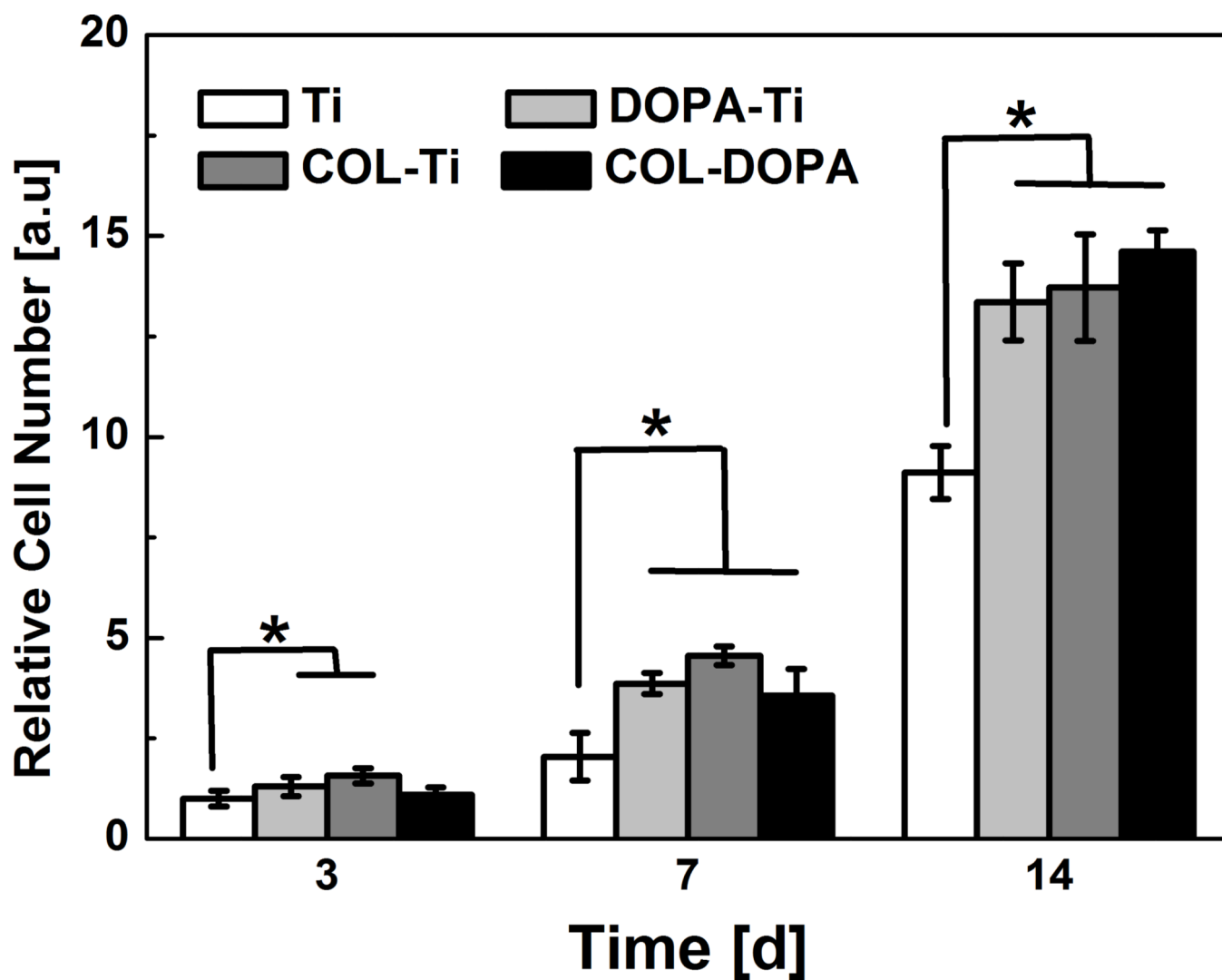


Fig. 6. MC3T3-E1 cell proliferation on titanium surface treated with different approaches. Relative cell number is normalized by the cell number on Ti group at day 3. * indicates statistically significant differences ($p < 0.05$) compared with Ti Group.

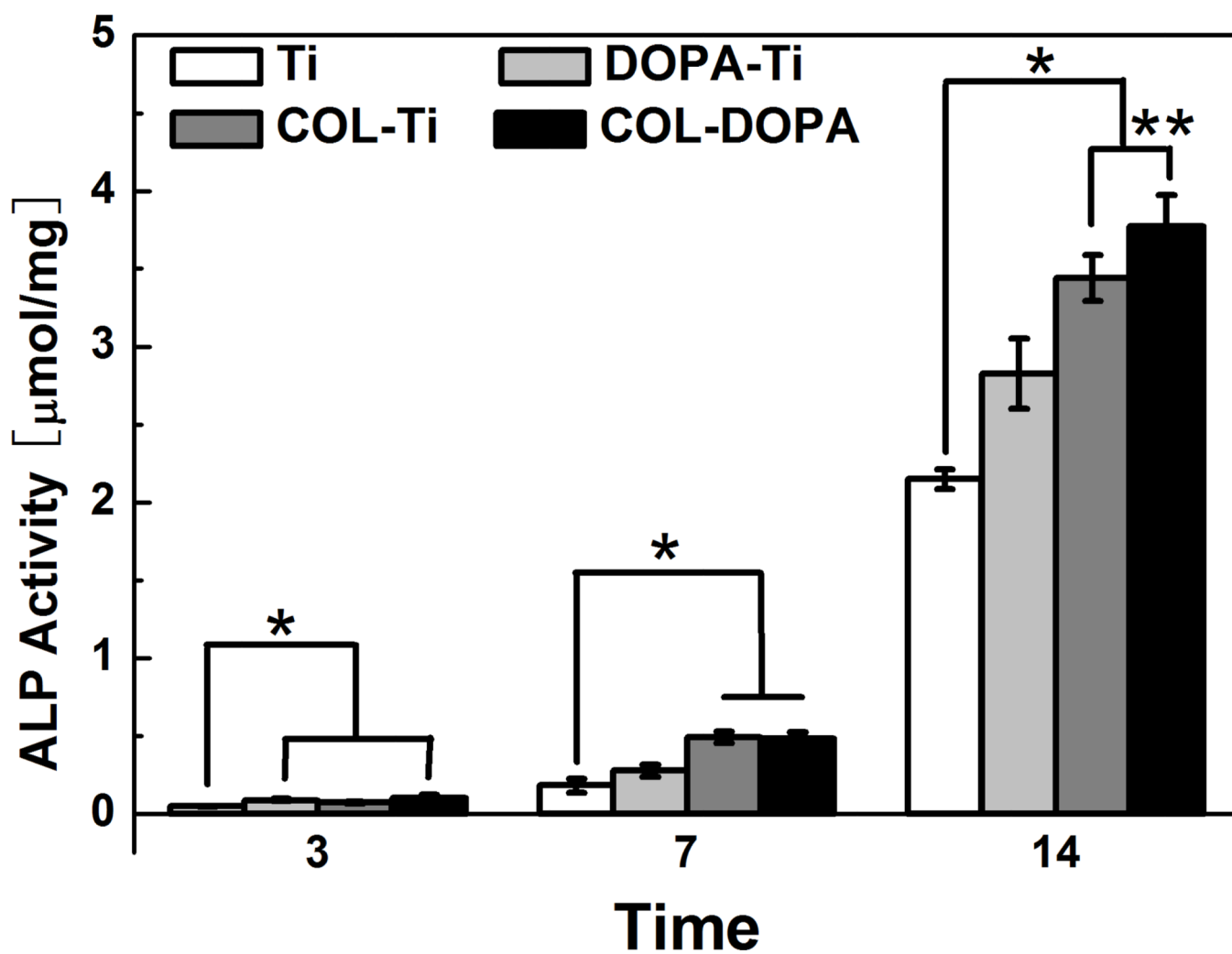


Fig. 7.

ALP expression by MC3T3-E1 on titanium surface treated with different approaches.

Relative cell number is normalized by the ALP activity on Ti group at day 3. * indicates statistically significant differences ($p < 0.05$) compared with Ti Group.

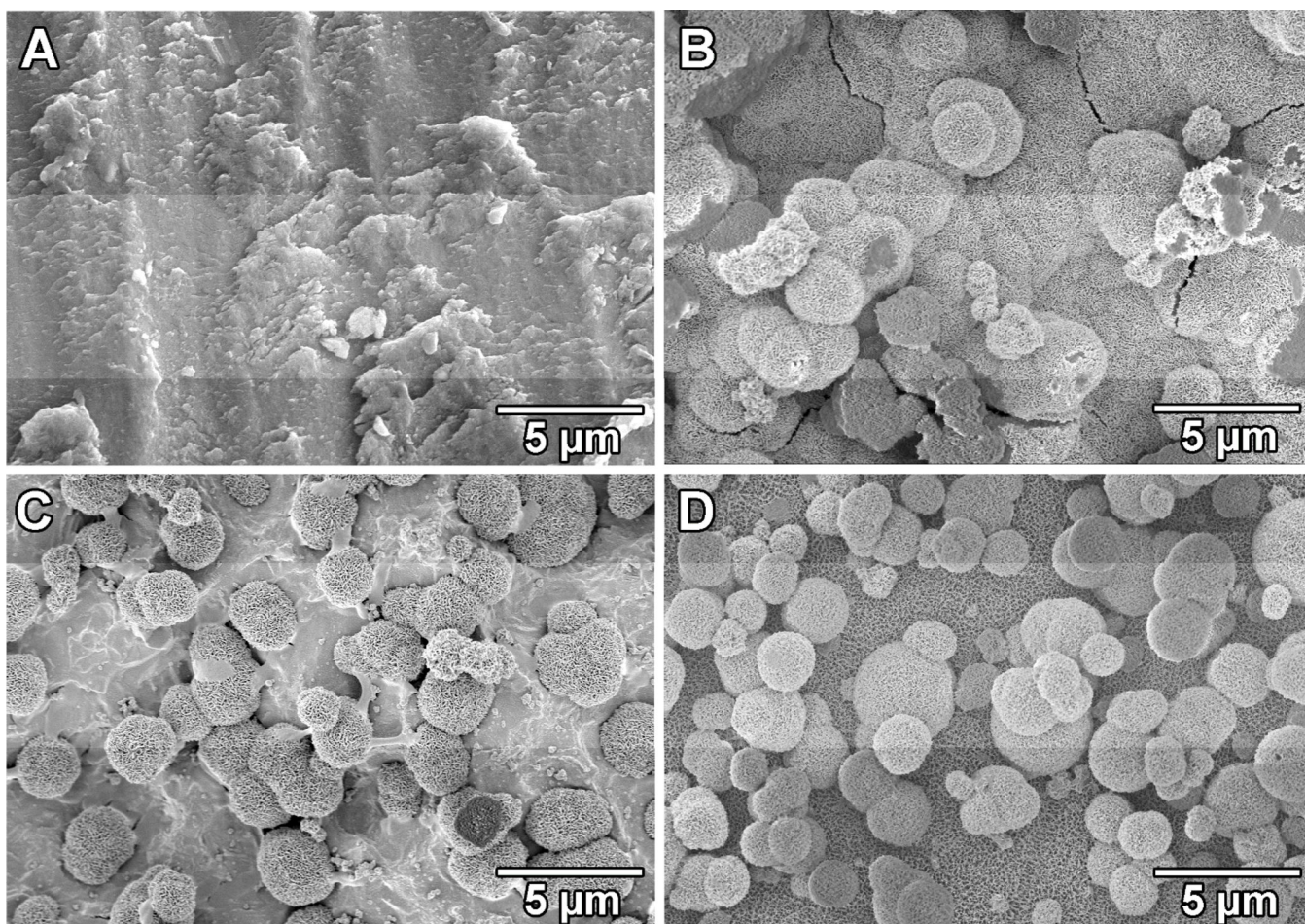


Fig. 8. Apatite coating formation on four types of titanium surfaces with different treatment: (A) Ti, (B) DOPA-Ti, (C) COL-Ti, and (D) COL-DOPA after soaking in SBF for 7 days with daily solution refreshment

Table 1

Atomic compositions of the surface before and after treatment by XPS

	Ti	C	N	O
Ti (Control)	3.91	70.13	2.04	22.79
DOPA	0	76.17	4.96	18.87
COL-DOPA	0	68.77	13.73	17.50
COL-Ti	2.84	63.37	11.57	25.06
Pure collagen	0	69.20	12.60	17.10

Author Manuscript

Author Manuscript

Author Manuscript

Author Manuscript